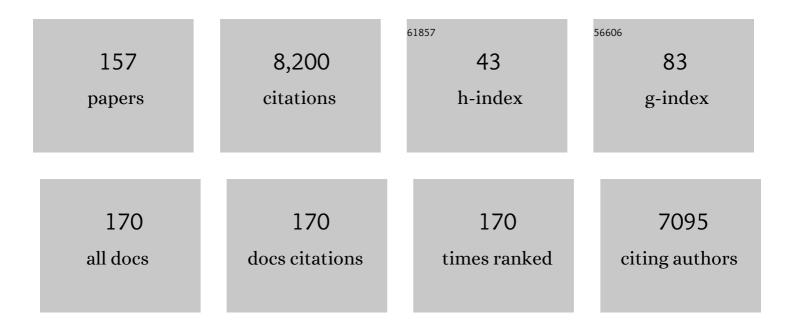
List of Publications by Year in descending order

Source: https://exaly.com/author-pdf/8601487/publications.pdf Version: 2024-02-01



SUSAN HURBADD

#	Article	IF	CITATIONS
1	Rapidly changing high-latitude seasonality: implications for the 21st century carbon cycle in Alaska. Environmental Research Letters, 2022, 17, 014032.	2.2	5
2	BASIN-3D: A brokering framework to integrate diverse environmental data. Computers and Geosciences, 2022, 159, 105024.	2.0	4
3	A Subseasonal Regime Approach for Assessing Intra-annual Variability of Evapotranspiration and Application to the Upper Colorado River Basin. Frontiers in Water, 2022, 3, .	1.0	Ο
4	Watershed zonation through hillslope clustering for tractably quantifying above- and below-ground watershed heterogeneity and functions. Hydrology and Earth System Sciences, 2022, 26, 429-444.	1.9	19
5	Surface parameters and bedrock properties covary across a mountainous watershed: Insights from machine learning and geophysics. Science Advances, 2022, 8, eabj2479.	4.7	12
6	A distributed temperature profiling system for vertically and laterally dense acquisition of soil and snow temperature. Cryosphere, 2022, 16, 719-736.	1.5	13
7	From legacy contamination to watershed systems science: a review of scientific insights and technologies developed through DOE-supported research in water and energy security. Environmental Research Letters, 2022, 17, 043004.	2.2	12
8	Variability of Snow and Rainfall Partitioning Into Evapotranspiration and Summer Runoff Across Nine Mountainous Catchments. Geophysical Research Letters, 2022, 49, .	1.5	6
9	Estimation of soil classes and their relationship to grapevine vigor in a Bordeaux vineyard: advancing the practical joint use of electromagnetic induction (EMI) and NDVI datasets for precision viticulture. Precision Agriculture, 2021, 22, 1353-1376.	3.1	15
10	Modeling the Impact of Riparian Hollows on River Corridor Nitrogen Exports. Frontiers in Water, 2021, 3, .	1.0	15
11	Geophysical Monitoring Shows that Spatial Heterogeneity in Thermohydrological Dynamics Reshapes a Transitional Permafrost System. Geophysical Research Letters, 2021, 48, e2020GL091149.	1.5	22
12	Influence of soil heterogeneity on soybean plant development and crop yield evaluated using time-series of UAV and ground-based geophysical imagery. Scientific Reports, 2021, 11, 7046.	1.6	18
13	Bedrock weathering contributes to subsurface reactive nitrogen and nitrous oxide emissions. Nature Geoscience, 2021, 14, 217-224.	5.4	18
14	Hysteresis Patterns of Watershed Nitrogen Retention and Loss Over the Past 50Âyears in United States Hydrological Basins. Global Biogeochemical Cycles, 2021, 35, e2020GB006777.	1.9	29
15	Meanders as a scaling motif for understanding of floodplain soil microbiome and biogeochemical potential at the watershed scale. Microbiome, 2021, 9, 121.	4.9	11
16	The Colorado East River Community Observatory Data Collection. Hydrological Processes, 2021, 35, e14243.	1.1	10
17	High-Resolution Spatio-Temporal Estimation of Net Ecosystem Exchange in Ice-Wedge Polygon Tundra Using In Situ Sensors and Remote Sensing Data. Land, 2021, 10, 722.	1.2	4
18	Integrated geophysical imaging of permafrost distribution across an Arctic watershed. , 2021, , .		0

2

#	Article	IF	CITATIONS
19	Field-scale estimation of soil properties from spectral induced polarization tomography. Geoderma, 2021, 403, 115380.	2.3	12
20	A hybrid data–model approach to map soil thickness in mountain hillslopes. Earth Surface Dynamics, 2021, 9, 1347-1361.	1.0	2
21	A deep learning hybrid predictive modeling (HPM) approach for estimating evapotranspiration and ecosystem respiration. Hydrology and Earth System Sciences, 2021, 25, 6041-6066.	1.9	8
22	Making a Water Data System Responsive to Information Needs of Decision Makers. Frontiers in Climate, 2021, 3, .	1.3	4
23	Differential C-Q Analysis: A New Approach to Inferring Lateral Transport and Hydrologic Transients Within Multiple Reaches of a Mountainous Headwater Catchment. Frontiers in Water, 2020, 2, .	1.0	24
24	Emerging technologies and radical collaboration to advance predictive understanding of watershed hydrobiogeochemistry. Hydrological Processes, 2020, 34, 3175-3182.	1.1	24
25	The Snowmelt Niche Differentiates Three Microbial Life Strategies That Influence Soil Nitrogen Availability During and After Winter. Frontiers in Microbiology, 2020, 11, 871.	1.5	32
26	Imaging of plant current pathways for non-invasive root Phenotyping using a newly developed electrical current source density approach. Plant and Soil, 2020, 450, 567-584.	1.8	24
27	Satellite-derived foresummer drought sensitivity of plant productivity in Rocky Mountain headwater catchments: spatial heterogeneity and geological-geomorphological control. Environmental Research Letters, 2020, 15, 084018.	2.2	20
28	Time-lapse monitoring of root water uptake using electrical resistivity tomography and mise-A-la-masse: a vineyard infiltration experiment. Soil, 2020, 6, 95-114.	2.2	27
29	Depth―and Timeâ€Resolved Distributions of Snowmeltâ€Driven Hillslope Subsurface Flow and Transport and Their Contributions to Surface Waters. Water Resources Research, 2019, 55, 9474-9499.	1.7	25
30	Sustaining Water Resources: Environmental and Economic Impact. ACS Sustainable Chemistry and Engineering, 2019, 7, 2879-2888.	3.2	32
31	Microbial communities across a hillslopeâ€riparian transect shaped by proximity to the stream, groundwater table, and weathered bedrock. Ecology and Evolution, 2019, 9, 6869-6900.	0.8	24
32	Investigating Microtopographic and Soil Controls on a Mountainous Meadow Plant Community Using Highâ€Resolution Remote Sensing and Surface Geophysical Data. Journal of Geophysical Research G: Biogeosciences, 2019, 124, 1618-1636.	1.3	23
33	Assessment of Spatiotemporal Variability of Evapotranspiration and Its Governing Factors in a Mountainous Watershed. Water (Switzerland), 2019, 11, 243.	1.2	20
34	A distributed temperature profiling method for assessing spatial variability in ground temperatures in a discontinuous permafrost region of Alaska. Cryosphere, 2019, 13, 2853-2867.	1.5	27
35	Challenges in Building an End-to-End System for Acquisition, Management, and Integration of Diverse Data From Sensor Networks in Watersheds: Lessons From a Mountainous Community Observatory in East River, Colorado. IEEE Access, 2019, 7, 182796-182813.	2.6	18
36	Predicting sedimentary bedrock subsurface weathering fronts and weathering rates. Scientific Reports, 2019, 9, 17198.	1.6	31

#	Article	IF	CITATIONS
37	Evaluating temporal controls on greenhouse gas (CHG) fluxes in an Arctic tundra environment: An entropy-based approach. Science of the Total Environment, 2019, 649, 284-299.	3.9	23
38	Landscape topography structures the soil microbiome in arctic polygonal tundra. Nature Communications, 2018, 9, 777.	5.8	105
39	Influence of Hydrological Perturbations and Riverbed Sediment Characteristics on Hyporheic Zone Respiration of CO <sub>2</sub> and N <sub>2</sub> . Journal of Geophysical Research G: Biogeosciences, 2018, 123, 902-922.	1.3	56
40	Depthâ€Resolved Physicochemical Characteristics of Active Layer and Permafrost Soils in an Arctic Polygonal Tundra Region. Journal of Geophysical Research G: Biogeosciences, 2018, 123, 1366-1386.	1.3	6
41	Biogenic sulfide control by nitrate and (per)chlorate – A monitoring and modeling investigation. Chemical Geology, 2018, 476, 180-190.	1.4	23
42	Remote Sensing to Uav-Based Digital Farmland. , 2018, , .		0
43	The East River, Colorado, Watershed: A Mountainous Community Testbed for Improving Predictive Understanding of Multiscale Hydrological–Biogeochemical Dynamics. Vadose Zone Journal, 2018, 17, 1-25.	1.3	115
44	Small-scale characterization of vine plant root water uptake via 3-D electrical resistivity tomography and mise-Ã-la-masse method. Hydrology and Earth System Sciences, 2018, 22, 5427-5444.	1.9	35
45	Deep Unsaturated Zone Contributions to Carbon Cycling in Semiarid Environments. Journal of Geophysical Research G: Biogeosciences, 2018, 123, 3045-3054.	1.3	15
46	Spatial and temporal variations of thaw layer thickness and its controlling factors identified using time-lapse electrical resistivity tomography and hydro-thermal modeling. Journal of Hydrology, 2018, 561, 751-763.	2.3	6
47	The Relative Importance of Saturated Silica Sand Interfacial and Pore Fluid Geochemistry on the Spectral Induced Polarization Response. Journal of Geophysical Research G: Biogeosciences, 2018, 123, 1702-1718.	1.3	4
48	Using strontium isotopes to evaluate the spatial variation of groundwater recharge. Science of the Total Environment, 2018, 637-638, 672-685.	3.9	23
49	Commemorating Dr. Gudmundur "Bo―Bodvarsson (1951–2006), a Leader of the Deep Unsaturated Flow and Transport Investigations. Water (Switzerland), 2018, 10, 18.	1.2	13
50	Integrated imaging of above and below ground properties and their interactions: A case study in East River Watershed, Colorado. , 2018, , .		3
51	Quantification of Arctic Soil and Permafrost Properties Using Ground-Penetrating Radar and Electrical Resistivity Tomography Datasets. IEEE Journal of Selected Topics in Applied Earth Observations and Remote Sensing, 2017, 10, 4348-4359.	2.3	23
52	Coincident aboveground and belowground autonomous monitoring to quantify covariability in permafrost, soil, and vegetation properties in Arctic tundra. Journal of Geophysical Research G: Biogeosciences, 2017, 122, 1321-1342.	1.3	42
53	Electrical and seismic response of saline permafrost soil during freeze - Thaw transition. Journal of Applied Geophysics, 2017, 146, 16-26.	0.9	59
54	Mapping snow depth within a tundra ecosystem using multiscale observations and Bayesian methods. Cryosphere, 2017, 11, 857-875.	1.5	28

#	Article	IF	CITATIONS
55	Coupled land surface–subsurface hydrogeophysical inverse modeling to estimate soil organic carbon content and explore associated hydrological and thermal dynamics in the Arctic tundra. Cryosphere, 2017, 11, 2089-2109.	1.5	12
56	Preface to the Special Issue of <i>Vadose Zone Journal</i> on Soil as Complex Systems. Vadose Zone Journal, 2016, 15, 1-3.	1.3	2
57	Quantifying shallow subsurface water and heat dynamics using coupled hydrological-thermal-geophysical inversion. Hydrology and Earth System Sciences, 2016, 20, 3477-3491.	1.9	16
58	Simulating bioclogging effects on dynamic riverbed permeability and infiltration. Water Resources Research, 2016, 52, 2883-2900.	1.7	57
59	Deep Vadose Zone Respiration Contributions to Carbon Dioxide Fluxes from a Semiarid Floodplain. Vadose Zone Journal, 2016, 15, 1-14.	1.3	24
60	Hierarchical Bayesian method for mapping biogeochemical hot spots using induced polarization imaging. Water Resources Research, 2016, 52, 533-551.	1.7	36
61	Time-lapse 3-D electrical resistance tomography inversion for crosswell monitoring of dissolved and supercritical CO2 flow at two field sites: Escatawpa and Cranfield, Mississippi, USA. International Journal of Greenhouse Gas Control, 2016, 49, 297-311.	2.3	22
62	Microbial Metagenomics Reveals Climate-Relevant Subsurface Biogeochemical Processes. Trends in Microbiology, 2016, 24, 600-610.	3.5	35
63	Identifying geochemical hot moments and their controls on a contaminated river floodplain system using wavelet and entropy approaches. Environmental Modelling and Software, 2016, 85, 27-41.	1.9	35
64	Estimating groundwater dynamics at a Colorado River floodplain site using historical hydrological data and climate information. Water Resources Research, 2016, 52, 1881-1898.	1.7	1
65	Analysis of laboratory data on ultrasonic monitoring of permeability reduction due to biopolymer formation in unconsolidated granular media. Geophysical Prospecting, 2016, 64, 445-455.	1.0	1
66	Thousands of microbial genomes shed light on interconnected biogeochemical processes in an aquifer system. Nature Communications, 2016, 7, 13219.	5.8	994
67	iMatTOUGH: An open-source Matlab-based graphical user interface for pre- and post-processing of TOUGH2 and iTOUGH2 models. Computers and Geosciences, 2016, 89, 132-143.	2.0	7
68	Geophysical estimation of shallow permafrost distribution and properties in an ice-wedge polygon-dominated Arctic tundra region. Geophysics, 2016, 81, WA247-WA263.	1.4	54
69	Microtopographic and depth controls on active layer chemistry in Arctic polygonal ground. Geophysical Research Letters, 2015, 42, 1808-1817.	1.5	44
70	Identifying multiscale zonation and assessing the relative importance of polygon geomorphology on carbon fluxes in an Arctic tundra ecosystem. Journal of Geophysical Research G: Biogeosciences, 2015, 120, 788-808.	1.3	74
71	Monitoring Arctic landscape variation by pole and kite mounted cameras. Proceedings of SPIE, 2015, , .	0.8	0
72	The emergence of hydrogeophysics for improved understanding of subsurface processes over multiple scales. Water Resources Research, 2015, 51, 3837-3866.	1.7	479

#	Article	IF	CITATIONS
73	Riverbed Clogging Associated with a California Riverbank Filtration System: An Assessment of Mechanisms and Monitoring Approaches. Journal of Hydrology, 2015, 529, 1740-1753.	2.3	41
74	Bayesian hierarchical approach and geophysical data sets for estimation of reactive facies over plume scales. Water Resources Research, 2014, 50, 4564-4584.	1.7	31
75	Geophysical monitoring and reactive transport simulations of bioclogging processes induced by <i>Leuconostoc mesenteroides</i> . Geophysics, 2014, 79, E61-E73.	1.4	12
76	Extrapolating active layer thickness measurements across Arctic polygonal terrain using LiDAR and <i>NDVI</i> data sets. Water Resources Research, 2014, 50, 6339-6357.	1.7	51
77	Bioclogging and Permeability Alteration by <i>L. mesenteroides</i> in a Sandstone Reservoir: A Reactive Transport Modeling Study. Energy & Fuels, 2013, 27, 6538-6551.	2.5	33
78	Reactive Transport Modeling of Induced Selective Plugging by <i>Leuconostoc Mesenteroides</i> in Carbonate Formations. Geomicrobiology Journal, 2013, 30, 813-828.	1.0	36
79	Identifying key controls on the behavior of an acidic-U(VI) plume in the Savannah River Site using reactive transport modeling. Journal of Contaminant Hydrology, 2013, 151, 34-54.	1.6	33
80	A new model for the biodegradation kinetics of oil droplets: application to the Deepwater Horizon oil spill in the Gulf of Mexico. Geochemical Transactions, 2013, 14, 4.	1.8	46
81	Quantifying and relating land-surface and subsurface variability in permafrost environments using LiDAR and surface geophysical datasets. Hydrogeology Journal, 2013, 21, 149-169.	0.9	127
82	Monitoring CO <sub>2</sub> Intrusion and Associated Geochemical Transformations in a Shallow Groundwater System Using Complex Electrical Methods. Environmental Science & Technology, 2013, 47, 314-321.	4.6	59
83	Effect of Dissolved CO <sub>2</sub> on a Shallow Groundwater System: A Controlled Release Field Experiment. Environmental Science & Technology, 2013, 47, 298-305.	4.6	168
84	Geochemical and geophysical responses during the infiltration of fresh water into the contaminated saprolite of the Oak Ridge Integrated Field Research Challenge site, Tennessee. Water Resources Research, 2013, 49, 4952-4970.	1.7	13
85	FIELD-SCALE GROUND-PENETRATING-RADAR TOMOGRAPHY AND UNCERTAINTY QUANTIFICATION THROUGH ENTROPY-BASED BAYESIAN INVERSION. , 2013, , .		0
86	Electrical Conductivity Imaging of Active Layer and Permafrost in an Arctic Ecosystem, through Advanced Inversion of Electromagnetic Induction Data. Vadose Zone Journal, 2013, 12, 1-19.	1.3	41
87	Hydrogeophysical investigations of the former S-3 ponds contaminant plumes, Oak Ridge Integrated Field Research Challenge site, Tennessee. Geophysics, 2013, 78, EN29-EN41.	1.4	30
88	Data-driven approach to identify field-scale biogeochemical transitions using geochemical and geophysical data and hidden Markov models: Development and application at a uranium-contaminated aquifer. Water Resources Research, 2013, 49, 6412-6424.	1.7	11
89	Petrophysical properties of saprolites from the Oak Ridge Integrated Field Research Challenge site, Tennessee. Geophysics, 2013, 78, D21-D40.	1.4	32
90	Remote Monitoring of Freeze–Thaw Transitions in Arctic Soils Using the Complex Resistivity Method. Vadose Zone Journal, 2013, 12, 1-13.	1.3	18

#	Article	IF	CITATIONS
91	Estimating active layer, ice-wedge, and permafrost property distributions in Arctic ecosystem using electrical conductivity imaging. , 2013, , .		1
92	Geophysical Monitoring of Foam Used to Deliver Remediation Treatments within the Vadose Zone. Vadose Zone Journal, 2012, 11, vzj2011.0160.	1.3	6
93	Estimation of Soil Hydraulic Parameters in the Field by Integrated Hydrogeophysical Inversion of Timeâ€Lapse Groundâ€Penetrating Radar Data. Vadose Zone Journal, 2012, 11, vzj2011.0177.	1.3	40
94	Visual Data Analysis as an Integral Part of Environmental Management. IEEE Transactions on Visualization and Computer Graphics, 2012, 18, 2088-2094.	2.9	6
95	Persistent Source Influences on the Trailing Edge of a Groundwater Plume, and Natural Attenuation Timeframes: The F-Area Savannah River Site. Environmental Science & Technology, 2012, 46, 4490-4497.	4.6	10
96	Calibration of a distributed flood forecasting model with input uncertainty using a Bayesian framework. Water Resources Research, 2012, 48, .	1.7	40
97	Estimating the spatiotemporal distribution of geochemical parameters associated with biostimulation using spectral induced polarization data and hierarchical Bayesian models. Water Resources Research, 2012, 48, .	1.7	23
98	Reactive facies: An approach for parameterizing fieldâ€scale reactive transport models using geophysical methods. Water Resources Research, 2012, 48, .	1.7	38
99	Long-term electrical resistivity monitoring of recharge-induced contaminant plume behavior. Journal of Contaminant Hydrology, 2012, 142-143, 33-49.	1.6	29
100	On parameterization of the inverse problem for estimating aquifer properties using tracer data. Water Resources Research, 2012, 48, .	1.7	18
101	Physicochemical Heterogeneity Controls on Uranium Bioreduction Rates at the Field Scale. Environmental Science & Technology, 2011, 45, 9959-9966.	4.6	79
102	Coupled modeling of hydrogeochemical and electrical resistivity data for exploring the impact of recharge on subsurface contamination. Water Resources Research, 2011, 47, .	1.7	35
103	Using complex resistivity imaging to infer biogeochemical processes associated with bioremediation of an uranium-contaminated aquifer. Journal of Geophysical Research, 2011, 116, .	3.3	79
104	ADVANCED SIMULATION CAPABILITY FOR ENVIRONMENTAL MANAGEMENT (ASCEM): AN OVERVIEW OF INITIAL RESULTS. Technology and Innovation, 2011, 13, 175-199.	0.2	6
105	Factors Governing Sustainable Groundwater Pumping near a River. Ground Water, 2011, 49, 432-444.	0.7	36
106	Lessons Learned from Bacterial Transport Research at the South Oyster Site. Ground Water, 2011, 49, 745-763.	0.7	20
107	Geophysical monitoring and reactive transport modeling of ureolytically-driven calcium carbonate precipitation. Geochemical Transactions, 2011, 12, 7.	1.8	54
108	3D induced-polarization data inversion for complex resistivity. Geophysics, 2011, 76, F157-F171.	1.4	41

#	Article	IF	CITATIONS
109	Advanced Remedial Methods for Metals and Radionuclides in Vadose Zone Environments. , 2010, , .		О
110	Effects of physical and geochemical heterogeneities on mineral transformation and biomass accumulation during biostimulation experiments at Rifle, Colorado. Journal of Contaminant Hydrology, 2010, 112, 45-63.	1.6	137
111	25. Detecting Perched Water Bodies Using Surface-Seismic Time-Lapse Traveltime Tomography. , 2010, , 415-428.		5
112	Characterization of Soil Water Content Variability and Soil Texture using GPR Groundwave Techniques. Journal of Environmental and Engineering Geophysics, 2010, 15, 93-110.	1.0	77
113	Understanding biogeobatteries: Where geophysics meets microbiology. Journal of Geophysical Research, 2010, 115, .	3.3	98
114	On the complex conductivity signatures of calcite precipitation. Journal of Geophysical Research, 2010, 115, .	3.3	42
115	Electrodic voltages accompanying stimulated bioremediation of a uraniumâ€contaminated aquifer. Journal of Geophysical Research, 2010, 115, .	3.3	7
116	Stochastic estimation of aquifer geometry using seismic refraction data with borehole depth constraints. Water Resources Research, 2010, 46, .	1.7	16
117	Three $\hat{\mathbf{e}}$ dimensional inversion of EM coupling contaminated spectral induced polarization data. , 2010, , .		0
118	Longâ€ŧerm timeâ€lapse surface and borehole electrical resistivity monitoring of natural recharge― induced contaminant plume behavior. , 2010, , .		0
119	Feedbacks Between Hydrological Heterogeneity and Bioremediation Induced Biogeochemical Transformations. Environmental Science & amp; Technology, 2009, 43, 5197-5204.	4.6	34
120	Mineral Transformation and Biomass Accumulation Associated With Uranium Bioremediation at Rifle, Colorado. Environmental Science & Technology, 2009, 43, 5429-5435.	4.6	101
121	Geophysical Monitoring of Coupled Microbial and Geochemical Processes During Stimulated Subsurface Bioremediation. Environmental Science & amp; Technology, 2009, 43, 6717-6723.	4.6	127
122	A stateâ€space Bayesian framework for estimating biogeochemical transformations using timeâ€lapse geophysical data. Water Resources Research, 2009, 45, .	1.7	19
123	Ground Penetrating Radar in Hydrogeophysics. Vadose Zone Journal, 2008, 7, 137-139.	1.3	34
124	Spectral induced polarization and electrodic potential monitoring of microbially mediated iron sulfide transformations. Journal of Geophysical Research, 2008, 113, .	3.3	49
125	Sulfur Isotopes as Indicators of Amended Bacterial Sulfate Reduction Processes Influencing Field Scale Uranium Bioremediation. Environmental Science & Technology, 2008, 42, 7842-7849.	4.6	21
126	Geophysical Monitoring of Hydrological and Biogeochemical Transformations Associated with Cr(VI) Bioremediation. Environmental Science & Technology, 2008, 42, 3757-3765.	4.6	44

#	Article	IF	CITATIONS
127	In Situ Long-Term Reductive Bioimmobilization of Cr(VI) in Groundwater Using Hydrogen Release Compound. Environmental Science & Technology, 2008, 42, 8478-8485.	4.6	86
128	A comparison between Gauss-Newton and Markov-chain Monte Carlo–based methods for inverting spectral induced-polarization data for Cole-Cole parameters. Geophysics, 2008, 73, F247-F259.	1.4	88
129	Joint inversion of crosshole radar and seismic traveltimes acquired at the South Oyster Bacterial Transport Site. Geophysics, 2008, 73, G29-G37.	1.4	78
130	Poreâ€scale spectral induced polarization signatures associated with FeS biomineral transformations. Geophysical Research Letters, 2007, 34, .	1.5	59
131	Calvanic interpretation of selfâ€potential signals associated with microbial sulfateâ€reduction. Journal of Geophysical Research, 2007, 112, .	3.3	15
132	Advanced Noninvasive Geophysical Monitoring Techniques. Annual Review of Earth and Planetary Sciences, 2007, 35, 653-683.	4.6	39
133	Inversion of tracer test data using tomographic constraints. Water Resources Research, 2006, 42, .	1.7	64
134	Introduction to special section on Hydrologic Synthesis. Water Resources Research, 2006, 42, .	1.7	5
135	Transport and biogeochemical reaction of metals in a physically and chemically heterogeneous aquifer. , 2006, 2, 220.		61
136	Joint inversion of geophysical and hydrological data for improved subsurface characterization. The Leading Edge, 2006, 25, 730-734.	0.4	22
137	HYDROGEOPHYSICAL PARAMETER ESTIMATION APPROACHES FOR FIELD SCALE CHARACTERIZATION. , 2006, , 9-44.		18
138	Hydrogeological Characterization Using Geophysical Methods. , 2006, , 14-1-14-52.		1
139	Evaluation of infiltration in layered pavements using surface GPR reflection techniques. Journal of Applied Geophysics, 2005, 57, 129-153.	0.9	94
140	Introduction to Hydrogeophysics. , 2005, , 3-21.		46
141	Geophysical Imaging of Stimulated Microbial Biomineralization. Environmental Science & Technology, 2005, 39, 7592-7600.	4.6	122
142	Soil moisture content estimation using ground-penetrating radar reflection data. Journal of Hydrology, 2005, 307, 254-269.	2.3	254
143	Low-frequency electrical response to microbial induced sulfide precipitation. Journal of Geophysical Research, 2005, 110, n/a-n/a.	3.3	89
144	Stochastic Forward and Inverse Modeling: The "Hydrogeophysical―Challenge. , 2005, , 487-511.		19

#	Article	IF	CITATIONS
145	Geochemical characterization using geophysical data and Markov Chain Monte Carlo methods: A case study at the South Oyster bacterial transport site in Virginia. Water Resources Research, 2004, 40, .	1.7	38
146	Measuring Soil Water Content with Ground Penetrating Radar: A Review. Vadose Zone Journal, 2003, 2, 476-491.	1.3	174
147	Measuring Soil Water Content with Ground Penetrating Radar: A Review. Vadose Zone Journal, 2003, 2, 476-491.	1.3	647
148	Mapping the volumetric soil water content of a California vineyard using high-frequency GPR ground wave data. The Leading Edge, 2002, 21, 552-559.	0.4	76
149	Breakthroughs in field-scale bacterial transport. Eos, 2001, 82, 417-417.	0.1	12
150	Hydrogeological characterization of the south oyster bacterial transport site using geophysical data. Water Resources Research, 2001, 37, 2431-2456.	1.7	167
151	Estimating the hydraulic conductivity at the south oyster site from geophysical tomographic data using Bayesian Techniques based on the normal linear regression model. Water Resources Research, 2001, 37, 1603-1613.	1.7	144
152	Ferrographic Tracking of Bacterial Transport in the Field at the Narrow Channel Focus Area, Oyster, VA. Environmental Science & Technology, 2001, 35, 182-191.	4.6	56
153	Hydrogeological parameter estimation using geophysical data: a review of selected techniques. Journal of Contaminant Hydrology, 2000, 45, 3-34.	1.6	132
154	Spatial correlation structure estimation using geophysical and hydrogeological data. Water Resources Research, 1999, 35, 1809-1825.	1.7	72
155	Estimation of permeable pathways and water content using tomographic radar data. The Leading Edge, 1997, 16, 1623-1630.	0.4	181
156	Ground-penetrating-radar-assisted saturation and permeability estimation in bimodal systems. Water Resources Research, 1997, 33, 971-990.	1.7	89
157	Paleozoic and Grenvillian Structures in the southern Appalachians: Extended interpretation of seismic reflection data. Tectonics, 1991, 10, 141-170.	1.3	13